

REPORT DOCUMENTATION PAGE		Form Approved OMB No. 0704-0188
<small>Public reporting burden for this collection of information is estimated to average 1 hour per response, including the time for reviewing instructions, searching existing data sources, gathering and maintaining the data needed, and completing and reviewing this collection of information. Send comments regarding this burden estimate or any other aspect of this collection of information, including suggestions for reducing this burden to Department of Defense, Washington Headquarters Services, Directorate for Information Operations and Reports (0704-0188), 1215 Jefferson Davis Highway, Suite 1204, Arlington, VA 22202-4302. Respondents should be aware that notwithstanding any other provision of law, no person shall be subject to any penalty for failing to comply with a collection of information if it does not display a current valid OMB control number. PLEASE DO NOT RETURN YOUR FORM TO THE ABOVE ADDRESS.</small>		
1. REPORT DATE (DD-MM-YYYY) 30-6-2007	2. REPORT TYPE FINAL	3. DATES COVERED (From - To) April 1,04-March 31,07
4. TITLE AND SUBTITLE Computational Analysis of Hybrid Two-Photon Absorbers with Excited State Absorbers		5a. CONTRACT NUMBER AFOSR FA9550-04-C-0036
		5b. GRANT NUMBER
		5c. PROGRAM ELEMENT NUMBER
6. AUTHOR(S) M. J. Potasek		5d. PROJECT NUMBER
		5e. TASK NUMBER
		5f. WORK UNIT NUMBER
7. PERFORMING ORGANIZATION NAME(S) AND ADDRESS(ES) A. J. Devaney Associates, Inc. 143 Newbury Street, Boston, MA 02116		8. PERFORMING ORGANIZATION REPORT NUMBER
9. SPONSORING / MONITORING AGENCY NAME(S) AND ADDRESS(ES) Air Force Office Scientific Research/NE 875 N. Randolph ATTN: Dr. Arje Nachman Ste. 325, RM 3112 Arlington, VA 22203		10. SPONSOR/MONITOR'S ACRONYM(S)
		11. SPONSOR/MONITOR'S REPORT NUMBER(S)
12. DISTRIBUTION / AVAILABILITY STATEMENT  unlimited <div style="text-align: right;">AFRL-SR-AR-TR-07-0474</div>		
13. SUPPLEMENTARY NOTES		
14. ABSTRACT This work represents the joint work of several groups including numerical calculations and experiments. Numerical calculations were performed for the propagation of a femtosecond laser beam through an optical path and a nonlinear absorber. The results were compared with experiments performed under similar conditions. There was excellent agreement between calculations and experiments at low input energy. However, further additions must be done to the calculation of the optical path for high input energy.		

15. SUBJECT TERM nonlinear absorbers, numerical simulations					
16. SECURITY CLASSIFICATION OF:			17. LIMITATION OF ABSTRACT none	18. NUMBER OF PAGES 26	19a. NAME OF RESPONSIBLE PERSON Dr. M. J. Potasek
a. REPORT U	b. ABSTRACT U	c. THIS PAGE U			19b. TELEPHONE NUMBER <i>(include area code)</i> 609-921-1338

Standard Form 298 (Rev. 8-98)
 Prescribed by ANSI Std. Z39.18

FINAL REPORT

30 June 2007

*“Computational Analysis of Hybrid Two-Photon
Absorbers with Excited State Absorption”*

ORGANIZATION:

A. J. Devaney Associates, Inc.
143 Newbury Street, Boston, MA 02116

PI:

M. J. Potasek

AFOSR Contract:

FA9550-04-C-0036

Dates:

April 1, 2004 to March 31, 2007

20071102542

Abstract

This work represents the joint work of several groups including numerical calculations and experiments. Numerical calculations were performed for the propagation of a femtosecond laser beam through an optical path and a nonlinear absorber. The results were compared with experiments performed under similar conditions. There was excellent agreement between calculations and experiments at low input energy. However, further additions must be done to the calculation of the optical path for high input energy.

Contents

Abstract.....	4
Table of Contents.....	5
1. Introduction.....	6
2. Description of the Test Case.....	7
2.1 Tasks.....	7
2.2 Simulation file format.....	8
3. Numerical Method Used for Propagation Through AF380.....	8
4. Results.....	11
4.1 Low Energy Case-10uJ.....	12
4.2 High Energy Case-1000uJ.....	13
5. Conclusions.....	16
6. References.....	16
7. Appendix.....	17

1. Introduction

Multiphoton absorption processes are useful in several applications. These applications include, but are not limited to, optical data storage [1]-[2], micro fabrication [3]-[7], photoconductors and photovoltaics [8], markers for genomes and proteins [9]-[10], biological and medical detectors [11]-[12], optical limiters [13]-[16], biomimetic electromagnetic devices [17], nanopatterning of inorganic/organic materials [18]-[19] and photomedicine/photodynamic therapy [20].

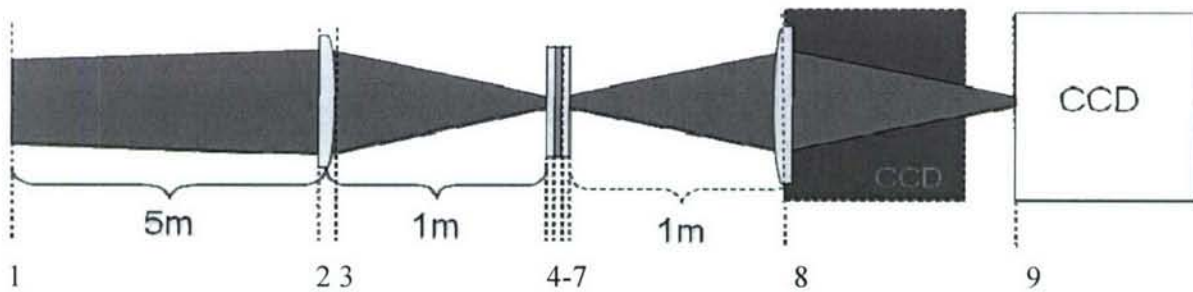
The wide range of applications of multiphoton absorption processes makes it particularly useful to have a detailed method for numerical investigations because some of the strongest two-photon absorbers are hybrid chromophores. These complex molecules exhibit a hybrid photo-activated energy level system in which the two-photon absorption (TPA) level is coupled to an excited state absorption (ESA) level. This hybrid arrangement creates a complex dynamical system in which the electron carrier concentration of every photo-activated energy level must be taken into account in order to determine the actual optical properties. Most traditional calculations of the laser matter interaction make simplifying assumptions about the optical field and the electron density states of the molecular system. We model propagation through two-photon materials and describe the numerical analysis of the complex interaction of the optical pulses with these hybrid systems. The numerical method calculates the spatiotemporal details of the electron population densities of each photo-activated energy level as well as the pulse shape in space and time.

The main topic of this effort was to coordinate a numerical simulation amongst a geographically and technically group of experts (See list below). The project involved a simulation of an optical path and propagation through a nonlinear absorber with experiments.

Good agreement was found between calculations and experiments at low input energy, but, at very high input energy it was determined that additional term, such as optical breakdown in air and lens, were required. This report describes the author's section of the project involving the propagation through the nonlinear absorber. It necessitated writing additional features in the propagation code including: (1) expressing the field in real units, (2) describing the field in terms of x, y, z, t and r, z, t and (3) inputting the field from a digitized field file.

2. Description of the Test Case

The test case involves simulations and comparison to experiments. A schematic diagram of the experimental set up for the test case is shown below.



Schematic diagram of the test case.

The nonlinear material is AF380. Test case parameters: laser pulse width 130 fs FWHM, laser wavelength 775 nm, laser energy 10 microJoule and 1 mJ, beam waist 2.5-3 mm $1/e^2$ radius, divergence ~ 100 microradians; sample thickness 1 mm AF380 film sandwiched between two glass slides, 1 mm each. Lens has a focal length of 1 m; lenses are either BK-7 or SF-11 Schott glass with 2.54 cm diameter. Data interchanges will be via flat ASCII files, SI units; in format 1pE14.21; space delimited by at least one column. Data interchange grid size: 256x256 (space, Cartesian) x 256 (time) or Cylindrical (256x256 space x time). Field magnitudes will be normalized such that peak amplitude is V/m to yield correct total energies.

2.1 Tasks:

Table of tasks

Task	Group	Activity
1	Bill Dennis UGA	model the initial Gaussian pulse and take care of propagation through all optical windows/elements.
2	Vance Hedin	model all free-space propagation steps throughout optical path.
3	Mary Potasek	model propagation through all two-photon materials within setup
4	Mark Walker	measurements
5	ALL	Final simulation results will be passed back to Mark for comparison to experimental data

Initially the data was passed from one group to another by CDs. Later a server was set up at Wright-Patterson AFB for the data exchange.

2.2 Simulation file format.

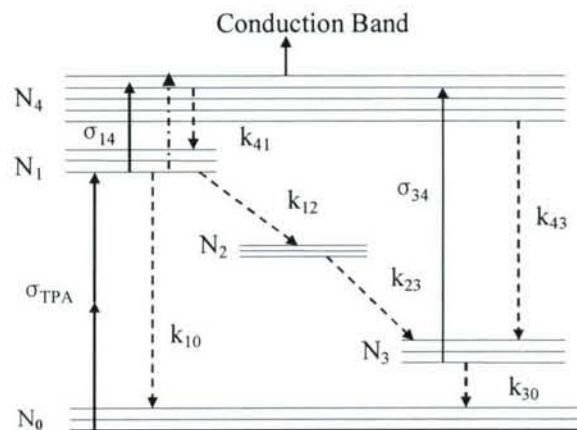
The field file is in the standard ASCII format (1PE24.15E3) and order (r,t or x,y,t). The params file has the following form:

Table for simulation file format.

Number	Description	Units
128	Number of space points	none
256	Number of time points.	none
1.0000000000000000E-003	The width of the spatial window	m
1.474970454238465E-012	The length of the time window	s
7.7500000000000000E-007	The center wavelength	m

3. Numerical method used for propagation through AF380

The energy level diagram for the AF380 is given below.



Schematic energy level diagram of the hybrid multiphoton absorber (AF380). The solid lines are the photo excitations, the dashed lines show the decay from the various electronic states and the dot-dashed line corresponds to the thermal excitation directly into the conduction band without any excited state absorption. The multiple horizontal lines represent the vibrational levels of the various electronic states. The parameters are $\sigma_{ipa} = 8.0 \text{ e-}21 \text{ cm}^4/\text{GW}$, $\sigma_{1,4} = 2.0 \text{ e-}17 \text{ cm}^2$, $\sigma_{3,4} = 2.0 \text{ e-}17 \text{ cm}^2$, $k_{10} = 0.5 \text{ e-}3 \text{ ps}^{-1}$, $k_{1,2} = 0.5 \text{ e-}2 \text{ ps}^{-1}$, $k_{2,3} = 0.29 \text{ e-}3 \text{ ps}^{-1}$, $k_{4,3} = 4.0 \text{ e-}9 \text{ ps}^{-1}$, $k_{3,0} = 0.34 \text{ e-}3 \text{ ps}^{-1}$, $\eta = 0.06$

These parameters are used in the rate equations to analyze all the carrier density distributions. The propagation equation is coupled to these rate equations, which is used to calculate the laser pulse intensity shape. Initially all of the carriers are assumed to be in the ground state (N_0) before the laser pulse enters the material. The energy levels have the following properties. N_0 is the ground state, N_1 is the first excited state reached by two-photon absorption, N_2 is an intermediate state between the first excited state and the fluorescing state N_3 . The intermediate state is attributed to an intramolecular transitional state in which the two-photon excitation rearranges itself from the D- π section of the molecule towards the acceptor region. Quantum mechanical calculations of the excited state electron density and molecular motion support this interpretation. The upper level N_4 is assumed to be the continuum (similar to a conduction band in semiconductors) that can be populated from either N_1 or N_3 . Free carrier generation was demonstrated by measurement of a nonlinear photocurrent using a thin film of the material placed between transparent conducting glasses. N_4 has a long lifetime.

The rate equations are given by

$$\begin{aligned}
\frac{dN_0}{dt} &= -\frac{\sigma_{tpa} I(t)^2 N_0}{2\hbar\omega_0} + k_{1,0}N_1 + k_{3,0}N_3 \\
\frac{dN_1}{dt} &= \frac{\sigma_{tpa} I(t)^2 N_0}{2\hbar\omega_0} (1-\eta) - k_{1,0}N_1 - k_{1,2}N_1 - \frac{\sigma_{1,4} I(t) N_1}{\hbar\omega_0} \\
\frac{dN_2}{dt} &= k_{1,2}N_1 - k_{2,3}N_2 \\
\frac{dN_3}{dt} &= k_{2,3}N_2 - k_{3,0}N_3 - \frac{\sigma_{3,4} I(t) N_3}{\hbar\omega_0} + k_{4,3}N_4 \\
\frac{dN_4}{dt} &= \frac{\sigma_{3,4} I(t) N_3}{\hbar\omega_0} - k_{4,3}N_4 + \eta \frac{\sigma_{tpa} I(t)^2 N_0}{2\hbar\omega_0} + \frac{\sigma_{1,4} I(t) N_1}{\hbar\omega_0}
\end{aligned}$$

where N_j is the electron number density of the state j , $\sigma_{j,k}$ is the absorption cross-section for electron pumping from the state j to the state k , and $k_{j,k}$ is the decay rate from the state j to the state k . The fraction of the two-photon population contributing to the photo-induced current is

given by the Boltzman distribution for electron $\eta = \left(1 + \frac{-\Delta E}{k_B T}\right)^{-1}$ where T is the temperature, k_B

is Boltzman's constant and ΔE is the energy gap between the two-photon state and the continuum level.

The rate equations are written in the following form and assumed to be in a moving coordinate system

$$\frac{d\vec{N}}{dt} = \hat{M}\vec{N} = \left[\hat{G} + \frac{I}{\hbar\omega_0}\hat{H} + \frac{I^2}{2\hbar\omega_0}\hat{F}\right]\vec{N}$$

where the matrix M is given by

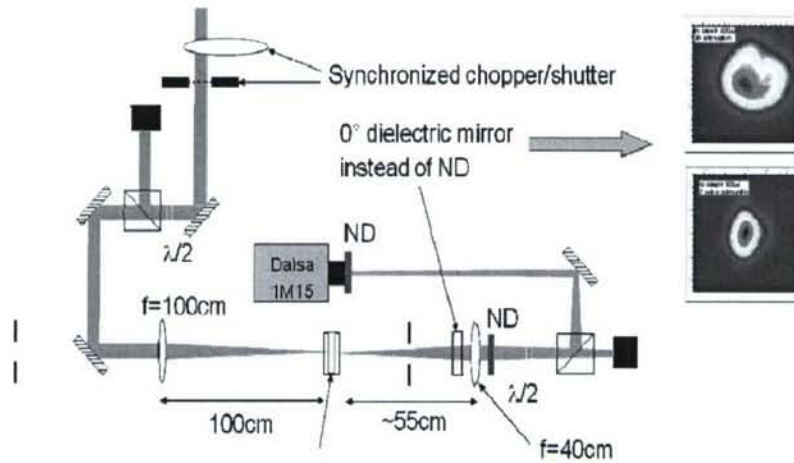
$$M = \begin{bmatrix} -\frac{\sigma_{tpa} I(t)^2}{2\hbar\omega_0} & k_{1,0} & 0 & k_{3,0} & 0 \\ \frac{\sigma_{tpa} I(t)^2}{2\hbar\omega_0}(1-\tilde{\eta}) & -k_{1,0}-k_{1,2}-\frac{\sigma_{1,4} I(t)}{\hbar\omega_0} & 0 & 0 & 0 \\ 0 & k_{1,2} & -k_{2,3} & 0 & 0 \\ 0 & 0 & k_{2,3} & -k_{3,0}-\frac{\sigma_{3,4} I(t)}{\hbar\omega_0} & k_{4,3} \\ \tilde{\eta} \frac{\sigma_{tpa} I(t)^2}{2\hbar\omega_0} & \frac{\sigma_{1,4} I(t)}{\hbar\omega_0} & 0 & \frac{\sigma_{3,4} I(t)}{\hbar\omega_0} & -k_{4,3} \end{bmatrix}$$

The matrix M is separated into three matrices for convenience. Thus G multiplies the constant decay terms, H multiplies terms dependent on the intensity and describes ESA, and F describes TPA. These matrices are given below.

$$G = \begin{bmatrix} 0 & k_{1,0} & 0 & k_{3,0} & 0 \\ 0 & -k_{1,0}-k_{1,2} & 0 & 0 & 0 \\ 0 & k_{1,2} & -k_{2,3} & 0 & 0 \\ 0 & 0 & k_{2,3} & -k_{3,0} & k_{4,3} \\ 0 & 0 & 0 & 0 & -k_{4,3} \end{bmatrix} \quad H = \begin{bmatrix} 0 & 0 & 0 & 0 & 0 \\ 0 & -\sigma_{1,4} & 0 & 0 & 0 \\ 0 & 0 & 0 & 0 & 0 \\ 0 & 0 & 0 & -\sigma_{3,4} & 0 \\ 0 & \sigma_{1,4} & 0 & \sigma_{3,4} & 0 \end{bmatrix} \quad F = \begin{bmatrix} -\sigma_{tpa} & 0 & 0 & 0 & 0 \\ \sigma_{tpa}(1-\tilde{\eta}) & 0 & 0 & 0 & 0 \\ 0 & 0 & 0 & 0 & 0 \\ 0 & 0 & 0 & 0 & 0 \\ \tilde{\eta}\sigma_{tpa} & 0 & 0 & 0 & 0 \end{bmatrix}$$

4. Results

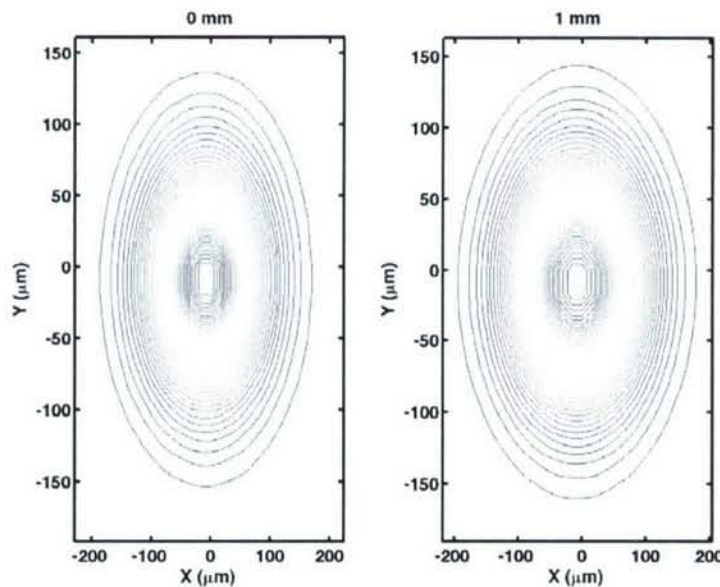
The following section describes the numerical and experimental results. The numerical results were obtained by calculating the laser propagation through the lens, air and first section of the cuvette (Prof. Dennis group), followed by propagation through AF380 (Potasek), and then propagation through the remainder of the optical path (Prof. Dennis group). The calculations were then compared with experiments (Mark Walker group). The following figures are from Potasek, except where noted. The results are divided into two energy regions: (1) low energy-10uJ and (2) high energy-1000uJ. A brief schematic diagram of the experimental set up is given in the figure below.



Experimental Set up (Mark Walker)

4.1 Low input energy-10 uJ

The numerical calculations and comparison with experiments are described next. In this case the input energy is 10uJ. The plots below show the calculated contour plots for the pulse propagation from the input to the material and the output from the material. As can be seen there is no pulse distortion.

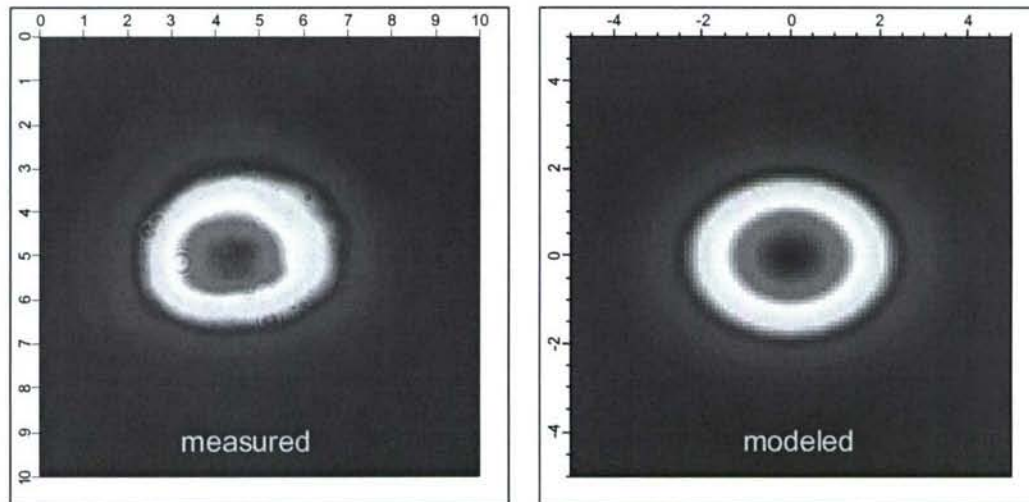


Calculated contour plots. Left side: $z=0$. Right side: $z=1$ mm.

The figure below shows a comparison between the numerical calculation and the experiment. As can be from the figure, there is good agreement between the calculation and the experiment.

Mod/Sim Comparison

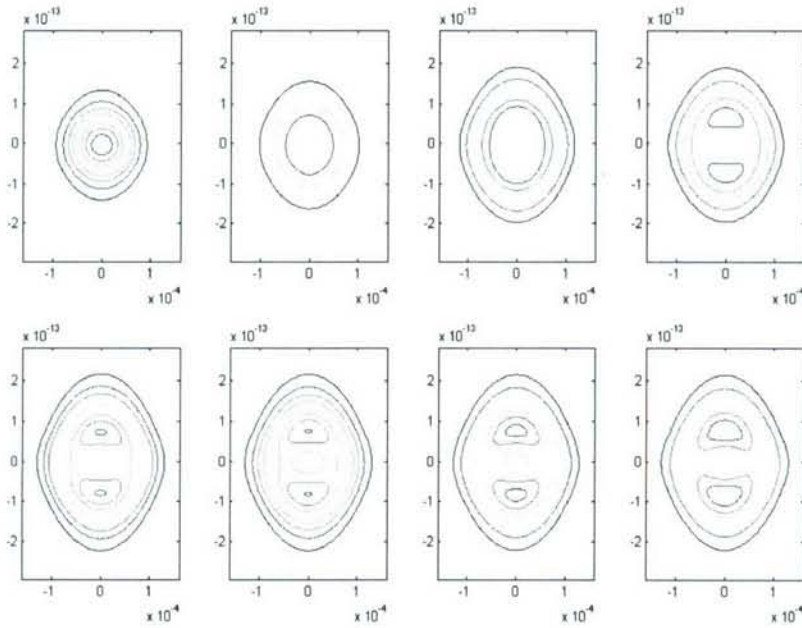
Time Integration of Input Pulse to Measured Beam Profile
dimensions are in mm



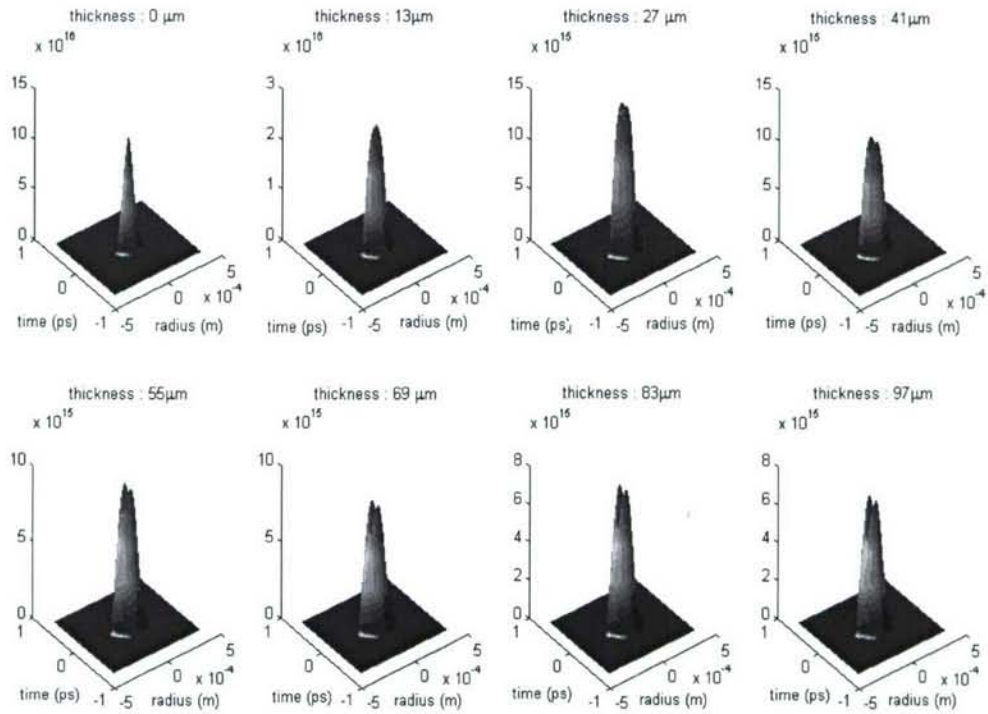
(From Mark Walker, MLPJ)

4.2 High Input Energy-1000uJ

The next section compares the numerical calculations with the experiments. The numerical calculations include the calculations from both the Dennis group and Potasek. It should be noted that at high input energy there is optical breakdown in the air and cuvette, which is not taken into account by the Dennis group at this time. The plots below show the calculated pulse shapes and contour plots as a function of propagation. It can be seen from the figures that the pulse splits in the temporal domain. This feature is not seen in the low energy case.

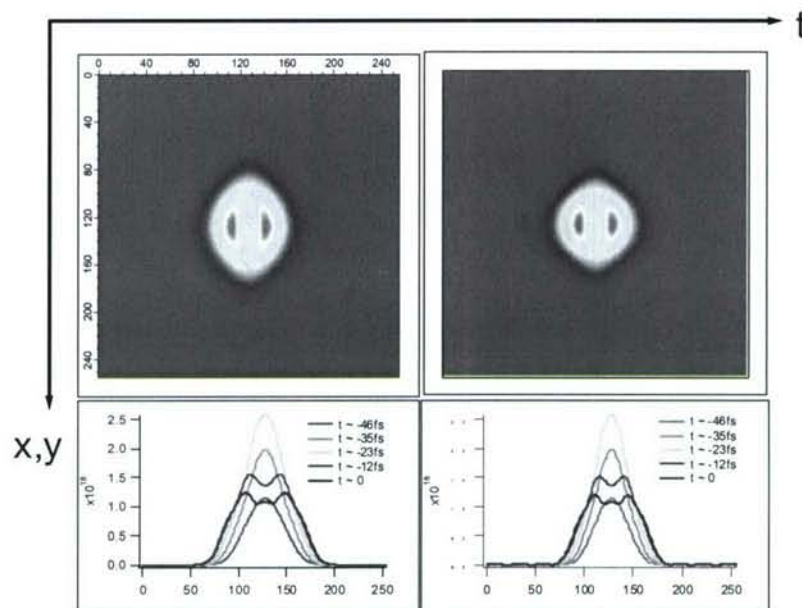


Calculated Contour Plots for Propagation through AF380 for x vs Time
as a Function of Distance (BK-7 lens) Input 1 mJ



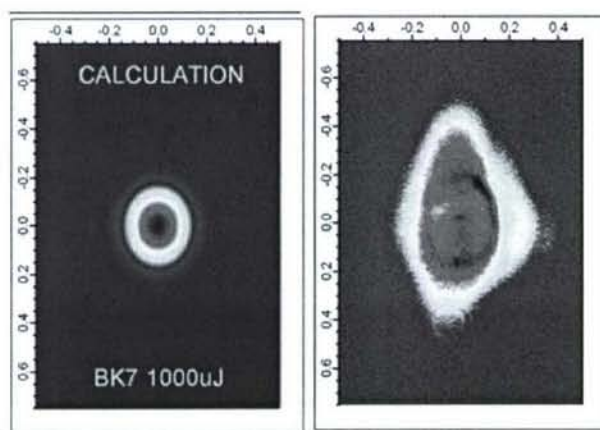
Corresponding Pulse Shapes for x versus t as a function of propagation distance.

These temporal features are seen in the comparison between calculations and experiments below.



Instantaneous beam profiles for x versus t. Left side: calculations. Right side: experiment (Mark Walker)

However, in the xy pulse shape there is significant difference between the calculations and the experiment. The figure below shows the calculation on the left and the experiment on the right. As can be seen from the figure the experimental pulse shape is significantly larger than the calculated one.



Comparison of beam shape at high input energy. (Mark Walker)

Additionally, there is a factor of two difference between the calculated experimental transmission.

5. Conclusions

Comparison of numerical calculations and experiments agreed well in the case of low input energy. However, for high input energy the agreement is not as good. The likely cause of the difference between experiment and calculation is probably due to neglect of ionization and plasma formation in the air between the lens and the AF380. Future calculations may need to include these effects.

6. References

1. H. E. Pudavar, M. P. Joshi, P. N. Prasad and B. A. Reinhardt, "High-density three-dimensional optical data storage in a stacked compact disk format with two-photon writing and single photon readout," *Appl. Phys. Lett.* **74**, 1338-1340 (1999).
2. B.H. Cumpston, S. Ananthavel, S. Barlow, D. L. Dyer, J.E. Ehrlich, L. L. Erskine, A. A. Heikal, S. M. Kuebler, I. Y. Lee, D. McCord-Maughon, J. Qin, H. Rockel, M. Rumi, X. L. Wu, S. R. Marder, and J. W. Perry, "Two-photon polymerization initiators for three-dimensional optical data storage and microfabrication," *Nature* **398**, 51-54 (1999).
3. W. Denk, J. H. Strickler and W. W. Webb, "Two-photon laser scanning fluorescence microscopy," *Science* **248**, 73-76 (1990).
4. S. Maruo and S. J. Kawata, "Two-photon-absorbed near-infrared photopolymerization for three-dimensional microfabridation," *J. Microelectromechanical Systems*, **7**, 411-422 (1998).
5. S. M. Kirkpatrick, J. W. Baur, C. M. Clark, L. R. Denny, B. R. Reinhardt, R. Kannan, M. O. Stone, "Holographic recording using two-photon-induced photopolymerization," *Appl. Phys. A* **69**, 461-464 (1999).
6. C. Diamond, Y. Boiko, and S. Esener, "Two-photon holography in a 3d photopolymer host-guest matrix," *Optics Express* **6**, 64-68 (2000).
7. S. Kawata, H. B. Sun, T. Tanaka, K. Takada, "Finer features for functional microdevices," *Nature* **412**, 697-698 (2001).
8. M. O. Stone, J. W. Baur, L. A. Sowards, and S. M. Kirkpatrick, "Ultrafast holographic recording of snake infrared pit tissue using two-photon induced photopolymerization," *Proc. SPIE*, **3934**, 36-42 (2000).
9. S. M. Kirkpatrick, E. K. Peterman, G. T. Anderson, J. E. Franklin, and J. W. Baur, "Nonlinear Photophysics and Charge Generation of Donor-Acceptor Two-Photon Absorbing Dyes," K. D. Belfield, S. J. Caracci, F. Kajzar, C. M. Lawson and A. T. Yeates, eds. *Proc. SPIE*, **4797**, 220-228 (2003).
10. F. K. Chan, R. M. Siegel, D. Zacharias, R. Swofford, K. L. Holmes, R. Y. Tsien, M. J. Lenardo, "Fluorescence resonance energy transfer analysis of cell surface receptor interactions

and signaling using spectral variants of the green fluorescent protein,” *Cytometry*. **44**, 361-368 (2001).

11. T. Misteli, D.L. Spector, “Applications of the green fluorescent protein in cell biology and biotechnology,” *Nat. Biotechnol.* **15**, 961-964 (1997).

12. M. E. Dickinson, E. Simbuerger, B. Zimmermann, C. W. Waters and S. E. Fraser, “Multiphoton excitation spectra in biological samples,” *J. Biomed Optics* **8**, 329-338 (2003).

13. B. J. Bacskaï, J. Skoch, G.A. Hickey, R. Allen and B. T. Hyman, “Fluorescence resonance energy transfer determinations using multiphoton fluorescence lifetime imaging microscopy to characterize amyloid-beta plaques,” *J. Biomed Optics* **8**, 368-375 (2003).

14. J. W. Perry, “Organic and metal-containing reverse saturable absorbers for optical limiters,” in *Nonlinear Optics of Organic Molecules and Polymers*, H. S. Nalwa and S. Miyata, Ed. Boca Raton, FL: CRC, 1997, pp.813-839.

15. G. S. He, J. D. Bhawalkar, C. F. Zhao, and P. N. Prasad, “Optical limiting effect in a two-photon absorption dye doped solid matrix,” *Appl. Phys. Lett.* **67**, 2433-2435 (1995).

16. M. G. Silly, L. Porres, O. Mongin, P. A. Chollet, M. Blanchard-Desce, “Optical limiting in the red-NIR range with soluble two-photon absorbing molecules,” *Chem. Phys. Lett.* **379**, 74-80 (2003).

17. M. Stone and R. Naik, “Applications-Biomimetic electromagnetic devices,” *Encyclopedia of Smart Materials*, John Wiley & Sons, New York, 2000.

18. L. L. Brott, R. R. Naik, D. J. Pikas, A. M. Kirkpatrick, D. W. Tomlin, P. W. Whitlock, S. J. Clarkson, and M. O. Stone, “Ultrafast holographic nanopatterning of biocatalytically formed silica,” *Nature* **413**, 291-293 (2001).

19. F. Stellacci, C.A. Bauer, T. Meyer-Friedrichsen, W. Wenseleers, V. Alain, S. M. Kuebler, S.J.K. Pond, Y. Zhang, S.R. Marder, J.W. Perry, “Laser and electron beam induced growth of nanoparticles for 2D and 3D metal patterning,” *Advan. Mat.* **14**, 194-198 (2002).

20. S. M. Kirkpatrick, C. Clark, R. L. Sutherland, “single state absorption spectra of novel nonlinear optical materials,” *Mat. Res. Soc. Symp. Proc.* Vol. 598 (2000).

7. Appendix

Personnel supported

PI:

M. J. Potasek

Collaborators:

- Drs. Sean Kirkpatrick, Chris Brewer and Mark Walker, WPAFB/ML
- Prof. Dennis, University of Georgia
- Dr. Erik Zeek, University of Georgia
- Dr. Tracey Bowen, Kirtland AFB
- Dr. Vance Hedin, Comcast

Publications:

No external reviewed publications

Three internal progress reports

Interactions/Transitions:

- a. Participation/presentations at meeting, conferences, etc
 - Presentation at Initial Meeting, AFOSR, Washington, DC, Jan 22, 2004
 - Presentation at Review Meeting, AT&T, Fairborn, Ohio, Dec 8, 2004
 - Presentation at Review Meeting, Kirtland AFB, N.M. Feb. 2, 2006
 - Numerous e-mail, phone discussions, and data exchange with Materials Lab, WPAFB and Bill Dennis and Erik Zeek, Univ of Georgia and others concerning the test case.
 - Numerical code and data exchange with Materials Lab, WPAFB and Bill Dennis and Erik Zeek, Univ of Georgia and others concerning the test case.

- b. Consultative and advisory functions to other laboratories and agencies
 - Meeting, discussions, phone calls,
 - Drs. Sean Kirkpatrick, Chris Brewer and Mark Walker, WPAFB/ML
 - Prof. Dennis, Univeristy of Georgia
 - Dr. Erik Zeek, Univeristy of Georgia
 - Dr. Tracey Bowen, Kirtland AFB
 - Dr. Vance Hedin, Comcast

- c. Transitions
 - Initial numerical code on multiphoton materials was transitioned to WPAFB.

New discoveries, inventions or patent disclosures:
None.